

---

# HALO: Long Horizon Latent Action Learning for General Robot Manipulation

---

Anonymous Author(s)

Affiliation

Address

email

## Abstract

1 Robotic manipulation often requires understanding long-horizon tasks guided by  
2 visual observations and language instructions. However, most existing Vision-  
3 Language-Action (VLA) models focus primarily on short-horizon tasks and over-  
4 look the rich historical video context, limiting their ability to perform complex,  
5 multi-step tasks. Moreover, these models often suffer from weak alignment be-  
6 tween pre-trained vision-language embeddings and robotic actions, which hinders  
7 the effective extraction of action-relevant priors from visual input and leads to inac-  
8 curate action generation. In this paper, we propose a novel Long Horizon Latent  
9 Action Learning framework for general robot manipulation, **HALO**, which enables  
10 robots to perform multi-step tasks by integrating long-term visual observations,  
11 multi-view camera images, and natural language instructions. To capture long-term  
12 dependencies, we propose to incorporate Qwen2.5-VL capable of processing long  
13 video and multi-view image sequences conditioned on natural language instructions.  
14 We further propose the State-Aware Latent Re-representation, which leverages  
15 robot states to query action-relevant features by selectively compressing and filter-  
16 ing the vision-language representations. The selected action-aligned embeddings  
17 are subsequently fed into an action expert, which predicts multi-step actions via  
18 a progressive denoising process. We have trained one of the largest VLA models  
19 with 10B trainable parameters, which is first pre-trained on one million diverse  
20 real-world robot episodes and fine-tuned across a wide range of downstream tasks.  
21 Experimental results on both simulated and real-world tasks demonstrate that our  
22 method achieves superior performance compared to prior state-of-the-art methods,  
23 particularly in long-horizon manipulation tasks.

24 

## 1 Introduction

25 With the rapid development of vision-language models (VLM) [1, 2, 3], robot manipulation policy  
26 models have seen significant progress. One of the most active areas in this domain is the Vision-  
27 Language-Action (VLA) model, which enables robots to perform complex tasks guided by natural  
28 language instructions [4, 5]. Notably, VLA models demonstrate strong generalization capabilities,  
29 even in environments that differ from the training distribution. This impressive performance is largely  
30 attributed to the powerful cross-modal understanding and reasoning abilities of VLMs, which allow  
31 the models to interpret diverse visual scenes and comprehend complex language commands within a  
32 unified framework.

33 The key to successfully training large Vision-Language-Action (VLA) models lies in effectively  
34 adapting vision-language models (VLMs) to a wide range of robotic manipulation tasks and de-  
35 signing task-specific components to generate accurate actions. Some approaches [4, 6] fine-tune  
36 VLMs to produce discrete action tokens, leveraging their large-scale pretrained knowledge while

37 preserving reasoning capabilities. Although these methods support generalized manipulation skills,  
38 the quantization process disrupts the continuity of actions. Other methods [5, 7, 8, 9] introduce a  
39 diffusion-based action head on top of the VLM. These models use vision-language embeddings ex-  
40 tracted by the VLM as conditional inputs to iteratively denoise probabilistic noise into future actions.  
41 However, because vision-language embeddings and actions originate from different modalities, these  
42 methods often suffer from weak cross-modal alignment. Directly fusing different modalities may  
43 introduce action-irrelevant information, such as background noises or visual distractors, into the  
44 decision process, and thus hinders accurate action prediction. Moreover, most existing models rely  
45 solely on the current frame to guide the robot, neglecting the importance of historical context. A  
46 single frame captures only the present state and overlooks temporal consistency, which can result  
47 in discontinuous or unstable actions. Incorporating historical information is essential, as it enables  
48 the model to generate more coherent action sequences and enhances its robustness in complex or  
49 dynamic environments.

50 To address these issues, we propose a novel Long **Horizon Latent Action Learning** framework for  
51 general **robot manipulation**, **HALO**, specially designed for long-horizon robotic tasks. **HALO**  
52 supports both extended historical frame sequences and multi-view camera inputs, and is capable  
53 of extracting action-relevant information from vision-language embeddings to guide future action  
54 generation. To fully leverage historical context, we adopt Qwen2.5-VL to process long video  
55 sequences and multi-view images. We select Qwen2.5-VL because of its strong ability to understand  
56 extended visual contexts, enabling the model to capture rich temporal and spatial information critical  
57 for long-horizon manipulation tasks. We further introduce a **Selective Spatial-Temporal Sampling**  
58 strategy that effectively integrates historical frames from multiple camera views. Processing all  
59 historical frames at high resolution incurs substantial computational cost, and not all frames contribute  
60 equally to decision-making. Our strategy is designed to minimize information loss while optimizing  
61 memory efficiency. Specifically, we reduce the resolution of historical frames from the primary  
62 view while preserving the full resolution of current-frame images across all views. This approach  
63 strikes a careful balance between leveraging rich historical context and retaining high-fidelity current  
64 observations, ultimately enhancing model performances in complex, long-horizon scenarios.

65 In addition, studies have shown that robot state information, such as joint angles and end-effector  
66 positions, shares the same modality as the action output, making it beneficial for action generation.  
67 For example,  $\pi_0$  leverages both robot state and vision-language embeddings to guide action prediction  
68 [5]. However, effectively fusing robot state with visual and language conditions remains challenging.  
69 Visual content is often high-dimensional and redundant compared to the compact action modality,  
70 which can lead to ineffective fusion and ultimately limit the accuracy of action prediction. To address  
71 this issue, we propose a **State-Aware Latent Re-representation** that leverages state information  
72 of robots to extract and refine the most action-relevant features from vision-language embeddings,  
73 thereby providing more accurate guidance for action generation. Specifically, we first propose a  
74 latent space generation method that computes the pairwise product between each token in the state  
75 embedding and each token in the vision-language embedding. This results in a large feature space  
76 that facilitates the search for action-relevant information. Then, we introduce a learnable mask that  
77 suppresses action-irrelevant information while preserving action-relevant cues from the latent space.  
78 This process transforms the vision-language embeddings into action-aligned embeddings that exhibit  
79 both modality consistency and strong action relevance.

80 We scale our model up to **10 billion trainable parameters** with optimized training strategies,  
81 which significantly enhances its capabilities in both perception and action generation. To enhance  
82 generalization, we adopt a step-by-step training pipeline that begins with large-scale pretraining and  
83 is followed by task-specific fine-tuning. In the pretraining phase, the model is trained on a large and  
84 diverse cross-embodiment robotic dataset comprising one million episodes, combining data from  
85 OXE [10] and the AgiBoT dataset [11]. This is followed by fine-tuning on three simulation datasets  
86 and real-world data collected using a Franka Research 3 robot setup. This training strategy enables  
87 the model to achieve state-of-the-art performance across a wide range of manipulation tasks and  
88 demonstrates strong generalization capabilities in handling long-horizon scenarios.

89 **2 Related Work**

90 **2.1 Vision-Language-Action Model**

91 Recently, relying on the powerful understanding and reasoning capabilities of Vision-Language-  
92 Models (VLM), Vision-Language-Action (VLA) models have made rapid progress, which integrates  
93 the action generation for adapting the robot manipulation tasks. For example, RT-2 [12] fine-tunes the  
94 VLM on large-scale vision-language data and robotic demonstration data using next-token prediction.  
95 It discretizes robotic actions into 256 binary values and represents them as independent tokens similar  
96 to text tokens. OpenVLA [4] adopts a similar discretization approach to fine-tune the Prismatic VLM  
97 [13] on the Open X-Embodiment dataset [10].  $\pi_0$  [5] consists of a PaliGemma model [14] and a  
98 separate action expert module, where the VLM is responsible for scene understanding, and the action  
99 expert module generates continuous actions through flow matching. Notably, while these models have  
100 shown some zero-shot ability, they usually use a single frame and ignore the temporal relationships,  
101 which may hinder the models generate consecutive actions and finally result in the failure of the task.

102 **2.2 Diffusion-based Robot Policy**

103 The diffusion model [15, 16, 17] is a mainstream model in the field of image generation. Recent  
104 studies [18, 19] have shown that diffusion models can effectively simulate various feasible trajec-  
105 tories that a robot may take to solve a given task. Diffusion policy [18] represents the visuomotor  
106 policy of robots as a conditional denoising diffusion process. Inspired by diffusion policies, Octo  
107 [20] incorporates a small diffusion head with a 3M parameters into a transformer-based backbone  
108 architecture to adapt the action outputs of different robots. RDT [21] proposes a pioneering diffusion  
109 foundation model for bimanual manipulation, with the diffusion model reaching 1 billion parameters.  
110 CogACT [7] first uses VLM to generate cognition tokens, then uses them as conditions to guide the  
111 diffusion model in generating actions that the robot can understand. However, these methods use  
112 vision-language embeddings that are not aligned with actions as conditions to guide action generation.  
113 In contrast, our model first aligns the vision-language embeddings with the state information of robots  
114 and achieves superior results.

115 **2.3 Long-Horizon Robot Manipulation**

116 In the field of robotic manipulation, learning long-horizon tasks has long been a persistent challenge  
117 [22, 23, 24, 25, 26, 27]. These tasks typically involve a series of fine-grained actions, each of  
118 which must account for physical constraints and their potential consequences, making them highly  
119 challenging for the policy model. For example, a long-horizon task may involve opening a microwave,  
120 placing a bowl of milk inside, closing the door, and setting the timer for 10 seconds. When task  
121 demonstrations are available, many studies, including PerAct [25], ARM [24], and VAPO[28],  
122 attempt to decompose complex long-horizon tasks into multiple stages by identifying sub-goals,  
123 thereby providing intermediate learning signals and mitigating the accumulation of action errors.  
124 However, these decomposition strategies often rely on task-specific knowledge, making them difficult  
125 to generalize to new tasks. Besides, ReflectVLM [26] aims to predict future world states and use  
126 these predictions to guide action selection and error correction, while DTP [27] attempts to adapt  
127 to long-horizon tasks by forecasting the trajectories of robots. UniVLA [23] incorporates historical  
128 actions into the input prompt, enabling the robot to learn from its own decisions and adapt to dynamic  
129 environments. Unlike these methods, our model leverages rich historical frame information to address  
130 long-horizon tasks. Information from historical frames is more informative, as it includes not only  
131 the actions of robots but also the effects of those actions on the environments, such as occlusion  
132 relationships caused by the manipulation of robots.

133 **3 Methodology**

134 Our goal is to develop a VLA model that enables different robots to accurately perform various  
135 tasks based on historical information, multi-view images, and language instructions. Specifically,  
136 given a long-horizon video input, multi-view images at the current single frame, and a language  
137 instruction, the proposed model predicts a temporal action sequence  $\{a_t, a_{t+1}, a_{t+2}, \dots, a_{t+s}\}$  to  
138 drive the robot to complete the corresponding tasks, where  $s$  is the number of predicted future

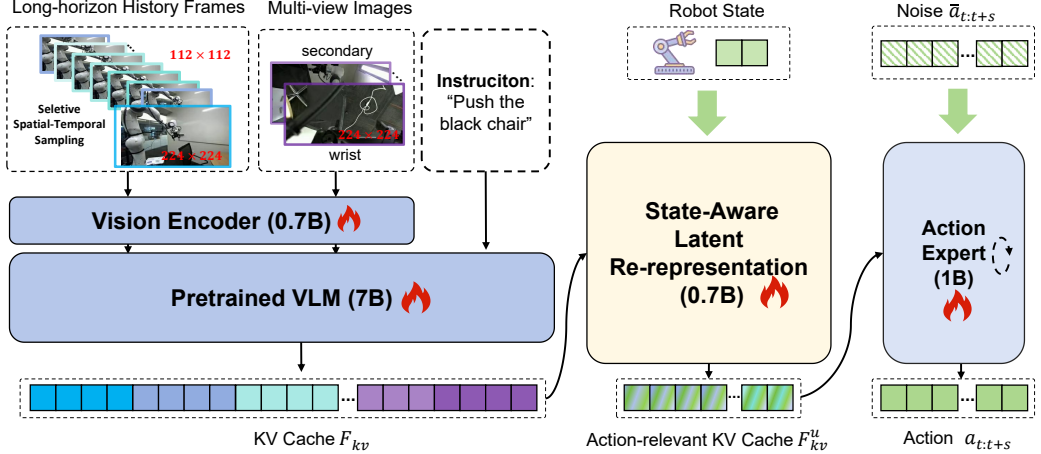


Figure 1: Overview of the proposed model **HALO**. **HALO** has 10 billion trainable parameters and can process long-horizon history frames (max to 8s when FPS is 10). To achieve the modality alignment between the vision-language embeddings and actions, the state-aware latent re-representation fuses the state information from robots and the vision-language embeddings.

139 steps. As shown in Figure 1, the proposed model consists of three components: the pretrained VLM,  
140 the State-Aware Latent Re-representation, and the Action Expert. Pretrained VLM is responsible  
141 for selecting the visual tokens most relevant to the language instruction from the long video and  
142 multi-view images. The State-Aware Latent Re-representation aligns the vision-language embeddings  
143 with actions, and the Action Expert decodes the desired action for the robot from noise based on the  
144 aligned embeddings.

### 145 3.1 Pretrained VLM for Long-Horizon Video Encoding

146 **Video Encoding.** Given a history video sequence  $\mathcal{V}$  which contains  $n$  frames and is obtained from  
147 the primary view:

$$\mathcal{V} = \{V_{t-n}^\downarrow, \dots, V_{t-3}^\downarrow, V_{t-2}^\downarrow, V_{t-1}^\downarrow, V_t\}, \quad (1)$$

148 where  $V^\downarrow$  and  $V_t$  denotes the downsampled frames and the  $t$ -th frame without downsampling,  
149 respectively. The primary view typically refers to a camera mounted at the front of the robot, which  
150 faces the task area. It provides the most critical and comprehensive perspective for observing the  
151 environment. The vision encoder from the pretrained vision-language model (VLM) is used to extract  
152 visual tokens  $F_v \in \mathbb{R}^{L_v \times H}$ , where  $L_v$  is the length of the video tokens and  $H$  is the hidden size.  
153 Because Qwen2.5-VL [29] is capable of understanding long videos exceeding one hour in duration  
154 by integrating dynamic frame rate (FPS) training with absolute time encoding, we choose it as the  
155 pretrained VLM. By adapting to varying frame rates, it can better capture the temporal dynamics of  
156 video content. To reduce the computational burden, we propose a selective spatial-temporal sampling  
157 strategy, which downsamples the resolution of historical frames while preserving high-resolution  
158 inputs for the current multi-view observations. Specifically, each frame of the video  $\mathcal{V}$  is first resized  
159 to  $112 \times 112$  and then is fed into the vision encoder. Although the resolution of historical frames is  
160 lower, their large number allows for complementary information during the feature extraction phase,  
161 thereby reducing information loss.

162 **Multi-View Image Encoding.** Since the resolution of the image of primary view is relatively low,  
163 some information may be lost. Therefore, the multi-view images  $\mathcal{V}$  at the current time  $t$ :

$$\mathcal{V}_m = \{V_{sec}, \dots, V_{wrist}\}, \quad (2)$$

164 are also fed into the vision encoder to mitigate this information loss, which keep the original size. The  
165 images from secondary view  $V_{sec}$  refers to images captured from alternative angles (e.g., side or top-  
166 down perspectives), which can help supplement the occluded regions from primary view. The wrist  
167 view is a camera mounted at the end of the arm of robot, which is near the gripper or tool and offers a  
168 close-up, detail, rich perspective that is useful for fine-grained manipulation tasks. Specifically, the

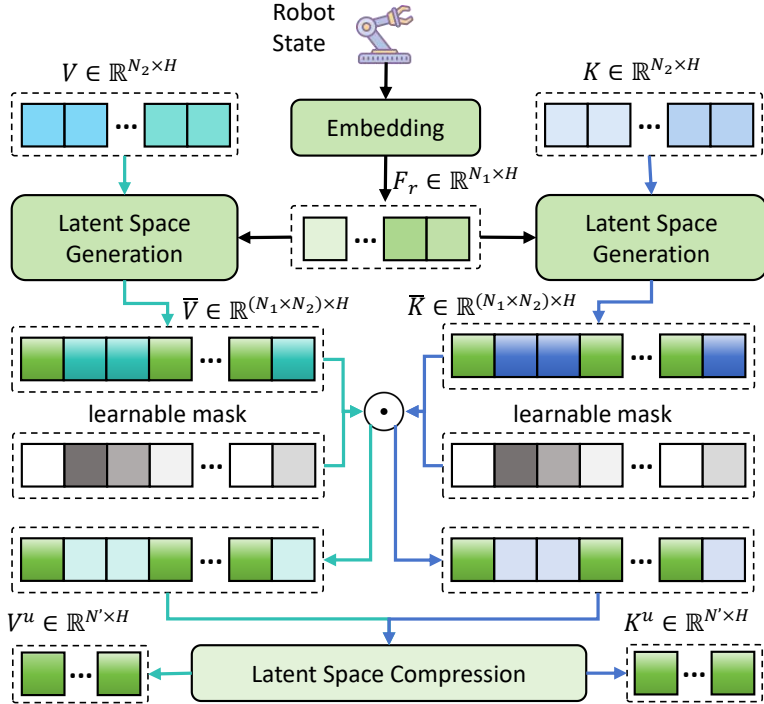


Figure 2: Illustration of the state-aware latent re-representation. The latent space generation calculate the product between each element from state embeddings and each element from the key token  $K$  or value token  $V$ . The learnable mask determines which information in the latent space is retained and which is suppressed. The latent space compression further compresses the latent space to filter out redundant information.

169 extracted multi-view tokens  $F_m \in \mathbb{R}^{L_m \times H}$  and video tokens  $F_v$  are concatenated and then jointly  
 170 fed into the large language model with the language tokens  $F_l$  to perform vision-language joint  
 171 perception:

$$F_{kv} = \text{VLM}(F_v, F_m, F_l), \quad (3)$$

172 where  $F_{kv}$  is the output KV cache.

### 173 3.2 State-Aware Latent Re-representation

174 In vision-language-action (VLA) model, there exists a significant gap between vision-language  
 175 embeddings and actions due to the inherently different modalities and representations of high-  
 176 level semantic information (e.g., language and vision) and low-level motor control signals. This  
 177 discrepancy makes it challenging for the model to directly translate abstract instructions and visual  
 178 cues into precise robotic actions. Therefore, effectively aligning these modalities is critical to  
 179 ensure that the robot can correctly understand the task and perform accurate, goal-directed behaviors.  
 180 However, current methods [5, 7, 9] suffer from weak alignment between actions and vision-language  
 181 embeddings. They usually use vision-language embeddings directly as conditions to predict future  
 182 actions, which may lead to irrelevant information in the embeddings (e.g., background features)  
 183 misguiding the action generation.

184 The state information of robots typically includes the joint angles or the position of the end-effector  
 185 at the current time step, and this modality is naturally aligned with the action space. Therefore, we  
 186 propose the Re-representation of State-Aware Latent, which leverages the state information of robots  
 187 to select action-aligned information from the redundant vision-language embeddings. Specifically, the  
 188 KV cache  $F_{kv} \in \mathbb{R}^{L \times 2N_2 \times H}$  output by the pretrained VLM is first split into keys  $F_k \in \mathbb{R}^{L \times N_2 \times H}$   
 189 and values  $F_v \in \mathbb{R}^{L \times N_2 \times H}$ , where  $L, N_2, H$  denotes the length of tokens, the number of heads and  
 190 the hidden size, respectively. They are not aligned with the action of the robot, so their representations  
 191 need to be updated to achieve alignment. We first propose to generate a larger action-relevant latent

192 space and then search within this space for features similar to actions. Specifically, as shown in Figure.  
 193 2, we perform head-wise outer-product fusion between the current state embeddings  $F_r \in \mathbb{R}^{N_1 \times H}$   
 194 of robots and the vision-language key embeddings, where  $N_1$  denotes the number of heads. Given  
 195 the key token  $K \in \mathbb{R}^{N_2 \times H}$  from  $F_k$ , the value token  $V \in \mathbb{R}^{N_2 \times H}$  from  $F_v$  and state embeddings  
 196  $F_r$ , the fused representation  $\bar{K} \in \mathbb{R}^{(N_1 \times N_2) \times H}$  and  $\bar{V} \in \mathbb{R}^{(N_1 \times N_2) \times H}$  are computed, respectively,  
 197 which capture rich inter-head interactions across modalities. Formally, it is defined as:

$$\begin{aligned}\bar{K}[i, j, :] &= F_r[i, :] \odot K[j, :], \\ \bar{V}[i, j, :] &= F_r[i, :] \odot V[j, :],\end{aligned}\quad (4)$$

198 where  $\odot$  denotes the element-wise product. Then, to extract action-relevant cues from the latent  
 199 space, we introduce a learnable mask for both the key tokens and value tokens, which adaptively  
 200 determines how much information to retain. Formally, this process can be written as:

$$\begin{aligned}K' &= M_k \odot K, \\ V' &= M_v \odot V,\end{aligned}\quad (5)$$

201 where  $M_k \in \mathbb{R}^{(N_1 \times N_2) \times H}$  and  $M_v \in \mathbb{R}^{(N_1 \times N_2) \times H}$  denotes the learnable mask for key token  
 202 and value token, respectively. Finally, to further compress the representation space, we propose a  
 203 latent space compression strategy to obtain re-encoded key embeddings  $K^u \in \mathbb{R}^{N' \times H}$  and value  
 204 embeddings  $V^u \in \mathbb{R}^{N' \times H}$ , where  $N'$  denotes the new number of heads.

### 205 3.3 Action Expert for Action Prediction

206 We use a conditional flow matching action expert [5] for fine-grained end-effector action generation,  
 207 which consists of a series of Transformer self-attention layers from pretrained large language model.  
 208 It takes the aligned vision-language embeddings as input condition to generate future multi-step  
 209 actions  $\{a_t, a_{t+1}, \dots, a_{t+s}\}$  and predicts actions through the progressive fusion of these embeddings  
 210 with noise. During inference, the Action Expert performs multiple denoising steps to progressively  
 211 decode the actions from noise.

## 212 4 Experiments

### 213 4.1 Implementation Details

214 Our HALO model is pretrained with OXE [30] and AgiBot dataset [11], consisting of 1.1 million  
 215 real-world robot episodes on a cluster of 32 A100 40G GPUs for 14 days. The VLM part of our  
 216 model is initialized from Qwen2.5VL-7B [29], and the full 10B model is trained in an end-to-end  
 217 fashion. Specifically, we use FSDP as our distributed training framework with hybrid sharding  
 218 strategy. Gradient checkpointing is used to reduce memory usage per batch. A gradient accumulation  
 219 step of 4 is utilized to boost batch size to 1280. We use LeRobot Dataset as our unified dataset format.  
 220 We further conduct inference experiment. The result shows that our model can support up to 30Hz of  
 221 control frequency on NVIDIA Geforce RTX A6000 GPUs.

### 222 4.2 Main Results

223 To demonstrate the effectiveness of our proposed model, we evaluate the model HALO across multiple  
 224 widely-used simulation benchmarks (including SIMPLER [31], LIBERO [32] and CALVIN [33])  
 225 and real-world scenarios. Besides, we further categorize the tasks into **Single-Step** and **Multi-Step**  
 226 tasks. The former requires executing only one atomic action (e.g., "pick", "put"), while the latter  
 227 involves a sequence of actions (e.g., "open" followed by "place").

#### 228 4.2.1 Manipulation Benchmark on SIMPLER

229 The SIMPLER [31] evaluation environment aims to bridge the real-to-sim control and visual gap. It  
 230 replicates real-world scenarios on the Google Robot and WidowX Robot. There are two real-to-sim  
 231 evaluation setups: **Visual Matching**, which aims to reduce the visual appearance gap between real  
 232 environments and raw simulation by overlaying real-world images onto simulation backgrounds,  
 233 and **Variant Aggregation**, which creates different simulation environment variants (e.g., different

Table 1: Comparison of our approach with existing VLA models across four tasks in two SIMPLER settings on the Google robot.

Google Robot	Method	Single-Step		Multi-Step		Average
		Pick Coke Can	Move Near	Open/Close Drawer	Open Top Drawer and Place Apple	
Visual Matching	RT-1 [34]	85.7%	44.2%	<b>73.0%</b>	6.5%	52.4%
	RT-1-X [10]	56.7%	31.7%	59.7%	<b>21.3%</b>	42.4%
	RT-2-X [10]	78.7%	<b>77.9%</b>	25.0%	3.7%	46.3%
	Octo-Base [20]	17.0%	4.2%	22.7%	0.0%	11.0%
	OpenVLA [4]	18.0%	56.3%	63.0%	0.0%	34.3%
	$\pi_0$ [5]	87.3%	35.0%	72.6%	16.0%	52.7%
<b>HALO (Ours)</b>		<b>88.0%</b>	53.8%	59.3%	26.9%	<b>57.0%</b>
Variant Aggregation	RT-1 [34]	<b>89.8%</b>	50.0%	32.3%	2.6%	43.7%
	RT-1-X [10]	49.0%	32.3%	29.4%	10.1%	30.2%
	RT-2-X [10]	82.3%	79.2%	35.3%	<b>20.6%</b>	54.4%
	Octo-Base [20]	0.6%	3.1%	1.1%	0.0%	1.2%
	OpenVLA [4]	60.8%	<b>67.7%</b>	28.3%	1.2%	39.3%
	$\pi_0$ [5]	85.2%	40.8%	42.1%	15.9%	46.0%
<b>HALO (Ours)</b>		86.2%	65.4%	<b>62.7%</b>	18.4%	<b>54.6%</b>

Table 2: Comparison of our approach with existing VLA models across four tasks in the SIMPLER (Visual Matching) setting on the WidowX robot.

WidowX Robot	Method	Multi-Step				Average
		Put Spoon on Towel	Put Carrot on Plate	Stack Green Block on Yellow Block	Put Eggplant in Yellow Basket	
Visual Matching	RT-1-X [34]	0.0%	4.2%	0.0%	0.0%	1.1%
	Octo-Base [20]	15.8%	12.5%	0.0%	41.7%	17.5%
	Octo-Small [20]	41.7%	8.2%	0.0%	56.7%	26.7%
	OpenVLA [4]	4.2%	0.0%	0.0%	12.5%	4.2%
	$\pi_0$ [5]	62.5%	<b>66.7%</b>	25.0%	12.5%	41.7%
	SpatialVLA [35]	16.7%	25.0%	29.2%	<b>100%</b>	42.7%
	CogACT [7]	<b>71.7%</b>	50.8%	15.0%	67.5%	51.3%
<b>HALO (Ours)</b>		54.2%	41.7%	<b>54.2%</b>	79.2%	<b>57.3%</b>

backgrounds, lightings, distractors, table textures) based on Visual Matching. We compare our model with the latest state-of-the-art VLA models under two evaluation settings. Table 1 summarizes the results of different VLA methods on two evaluation settings of the Google robot dataset. Our model achieves state-of-the-art performance in both settings, with 55.1% on **Visual Matching** and 54.6% on **Variant Aggregation**. Specifically, compared to  $\pi_0$ , our model achieves substantial improvements on multi-step tasks, outperforming it by 2.4% and 8.6% on **Visual Matching** and **Variant Aggregation**, respectively. Moreover, despite having fewer parameters (10B vs 55B), our model surpasses the closed-source RT-2-X in terms of success rate.

Table 2 summarizes the results of different methods on the WidowX robot. Our model also achieves the highest success rate, significantly outperforming other approaches. The tasks for this robot often involve multiple atomic actions and can thus be considered as multi-step tasks. For example, "put spoon on towel" requires first executing a pick action, followed by a put action. As shown in Table 2, our method achieves an overall improvement of 6% over  $\pi_0$ , demonstrating its ability to effectively extract task-relevant motion cues from historical information for more accurate action generation. Moreover, we observe that our model is capable of self-correction by leveraging historical context. For instance, when performing the "stack block" task, if it fails to grasp the green block on the first attempt, it continues to retry, with each subsequent attempt becoming more accurate.

#### 4.2.2 Manipulation Benchmark on LIBERO

The LIBERO [32] benchmark consists of four task suites, which are designed to study lifelong learning in robotic manipulation. We perform experiments on four task suites, each comprising

Table 3: Comparison of our approach with existing VLA models on the LIBERO simulation environments.

Method	Single-Step		Multi-Step			Average
	LIBERO-Goal	LIBERO-Object	LIBERO-Spatial	LIBERO-Long		
Diffusion Policy [18]	68.3%	92.5%	78.3%	50.5%	72.4%	
Octo [20]	84.6%	85.7%	78.9%	51.1%	75.1%	
OpenVLA [4]	79.2%	88.4%	84.7%	53.7%	76.5%	
TraceVLA [6]	75.1%	85.2%	84.6%	54.1%	74.8%	
RDT [21]	68.2%	77.8%	60.2%	29.0%	58.8%	
$\pi_0$ [5]	94.0%	<b>97.8%</b>	91.4%	85.4%	92.2%	
<b>HALO (Ours)</b>	<b>94.3%</b>	97.4%	<b>92.0%</b>	<b>85.6%</b>		<b>92.3%</b>

254 10 tasks with 50 human-teleoperated demonstrations. Specifically, **LIBERO-Spatial**, **LIBERO-**  
 255 **Object** and **LIBERO-Goal** evaluate the understanding of the spatial relationships, object types  
 256 and different task-oriented behaviors, respectively. **LIBERO-Long** test the ability to generalize the  
 257 long-horizon tasks with different objects, layouts and goals. Our model is fine-tuned on the mixed  
 258 LIBERO dataset for  $30k$  steps with a batch size of 128. Additionally, to ensure a fair comparison, we  
 259 reproduce the results of  $\pi_0$  on the LIBERO benchmark. Since LIBERO-Object, LIBERO-Spatial, and  
 260 LIBERO-Long contain multi-step instructions, we categorize them as **Multi-Step** dataset. Table 3  
 261 compares the performance of different VLA models on the LIBERO dataset. Our model achieves the  
 262 highest average success rate, surpassing existing state-of-the-art methods. Specifically, on the Multi-  
 263 Step datasets, our model outperforms  $\pi_0$  by 0.2% on LIBERO-Long and 0.6% on LIBERO-Spatial,  
 264 demonstrating that historical information can effectively guide the robot to perform accurate actions.

Table 4: Comparison of our approach with existing VLA models on the **ABC**→**D** subset of CALVIN benchmark. We report the success rates as well as the average number of completed tasks per evaluation sequence (with a maximum of 5 tasks).

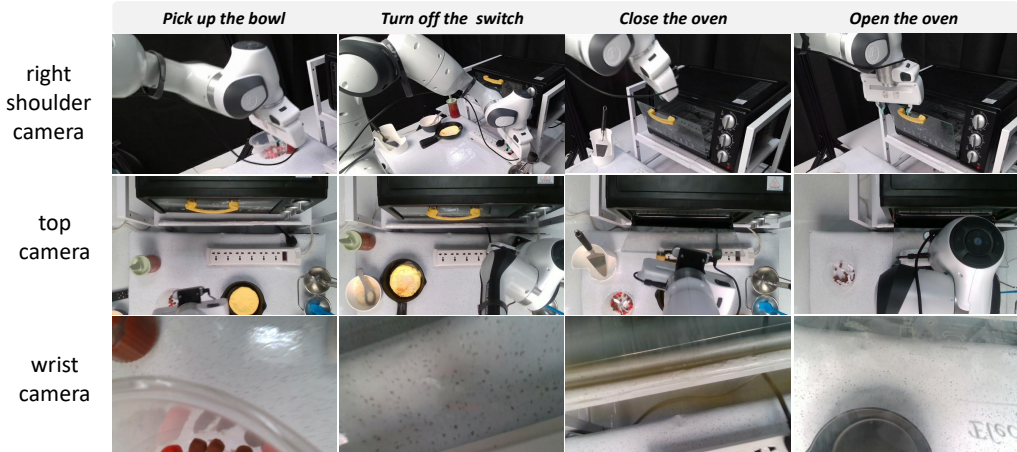
Method	Robot Data Only	Tasks completed in a row					Avg. Len.
		1	2	3	4	5	
MCIL [36]		0.304	0.013	0.002	0.000	0.000	0.31
Diffusion Policy [18]		0.402	0.123	0.026	0.008	0.000	0.56
RT-1 [34]		0.533	0.222	0.094	0.038	0.013	0.90
HULC [37]	✓	0.418	0.165	0.057	0.019	0.011	0.67
MT-R3M [38]		0.529	0.234	0.105	0.043	0.018	0.93
RoboFlamingo [39]		0.824	0.619	0.466	0.331	0.235	2.47
$\pi_0$ [5]		0.842	0.614	0.442	0.316	0.216	2.43
<b>HALO (Ours)</b>		0.848	0.638	0.443	0.323	0.234	2.49

#### 265 4.2.3 Manipulation Benchmark on CALVIN

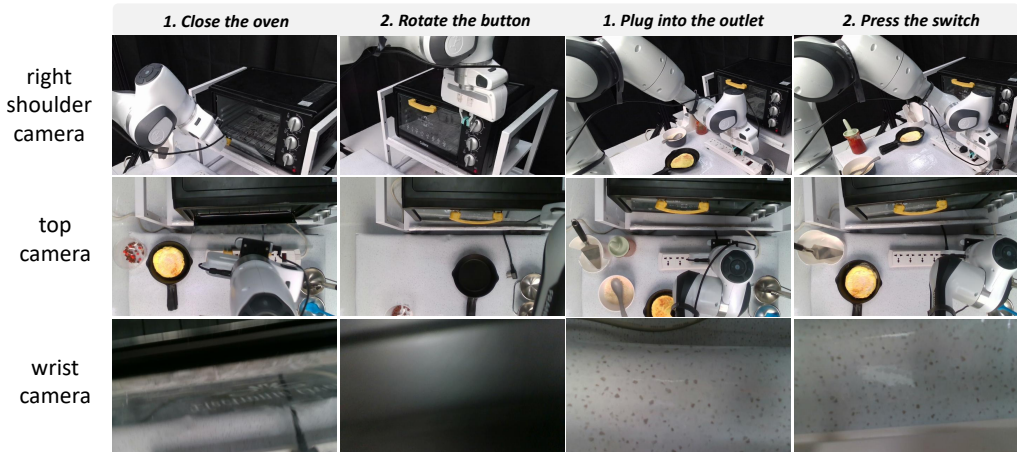
266 CALVIN [33] is a challenging simulated benchmark and aims to learn language-conditioned policy  
 267 for long-horizon robot manipulation tasks. It contains 34 tasks and the environment use the Franka  
 268 Emika Panda robot with a parallel-jaw gripper to perform the task. We conduct experiments on the  
 269 subset **ABC**→**D**, where A, B, C, and D represent different environments with variations in desk  
 270 colors and object configurations. In this setting, **ABC**→**D** denotes training on data from environments  
 271 A, B, and C, and testing on environment D, which serves as a zero-shot evaluation. The evaluation  
 272 consists of a set of 1,000 unique instruction chains, each comprising five consecutive tasks, designed  
 273 to comprehensively assess the generalization capability of the policy. Our model is finetuned on  
 274 the CALVIN training set for  $120k$  steps with a batch size of 128. Meanwhile, we also finetune  $\pi_0$   
 275 on CALVIN using the same settings for a fair comparison. The results in Table 4 demonstrate the  
 276 state-of-the-art performance of our method on long-horizon tasks with only using robot data. Under  
 277 the same training settings, our model outperforms  $\pi_0$ , exceeding it by 0.06 in terms of the average  
 278 number of completed tasks. Notably, by effectively leveraging historical information, our model is  
 279 capable of handling complex, long-horizon manipulation tasks.

Table 5: Comparison of our approach with existing VLA models in real-world scenarios with the Franka Robot.

Method	Single-Step				Multi-Step		Average
	T1	T2	T4	T8	T3 → T5	T6 → T7	
OpenVLA [4]	2/20	0	0	0	0	0	2/100
$\pi_0$ [5]	15/20	12/20	12/20	11/20	2/10	2/10	54/100
<b>Ours</b>	19/20	17/20	19/20	18/20	8/10	7/10	88/100



(a) single step



(b) multiple steps

Figure 3: Real-world evaluation of the long-horizon task "*Heat the Food*" using the Franka robot. The task includes two scenarios: (a) the target object (a pot) remains visible throughout the process, and (b) the target becomes occluded in the final step after being placed in the oven at the beginning.

#### 280 4.2.4 Real-World Evaluation with Franka Robot

281 **Self-collected Data.** We conduct experiments on the Franka robot, which has 7 DoFs and is equipped  
282 with a 1-DoF gripper.

283 **Training and Evaluation Details.** The implementation details trained on the real-world dataset are  
284 consistent with the fine-tuning in the simulation environment. Besides, we define 8 primitive tasks for  
285 **Single-Step** and **Multi-Step** for real-world evaluation: *Pick Bowl* (**T1**), *Turn off the switch* (**T2**), *Pick*

286 *Brush(T3), Open Oven(T4), Spread Sauce (T5), Plug into the Outlet (T6), Press the Switch (T7) and*  
287 *Close Oven (T8).*

288 **Results.** Table 5 summarizes the results of our model compared with OpenVLA and  $\pi_0$ . Our results  
289 demonstrate state-of-the-art performance on both single-step and multi-step tasks. Specifically, our  
290 model achieves a 60% and 50% higher success rate than  $\pi_0$  on the two-step task T3 → T5 and T6 →  
291 T7, respectively, which demonstrates the advantage in handling long-horizon tasks.

Table 6: Impact of each component. **Frozen VLM**, **MF** and **SALR** denotes the weights pretrained on robot dataset, the multiple frames and the State-Aware Latent Re-representation, respectively.

Frozen VLM	MF	SALR	Put Spoon on Towel	Put Carrot on Plate	Stack Green Block on Yellow Block	Put Eggplant in Yellow Basket	Average
✓	✓	✓	41.7%	50%	12.5%	16.7%	30.3%
			54.2%	45.8%	37.5%	29.2%	41.7%
			66.7%	50%	16.7%	45.8%	44.8%
✓	✓	✓	54.2%	41.7%	54.2%	79.2%	57.3%
✓	✓	✓	4.2%	0	0	0	1.1%

### 292 4.3 Ablation Study

293 We conduct ablation experiments on the WidowX robot from the SIMPLER simulated environment  
294 and report the average manipulation accuracy. **MF** means the multiple historical frames is use.  
295 **Pretrain** means the HALO is firstly pretrained on large-scale robot dataset and finetuned on the  
296 WidowX robot. **SALR** means the state-aware latent re-representation. Note that without using **MF**,  
297 only the current frame is used. Without **SALR**, a simple MLP is applied to convert the number of  
298 heads. As shown in Table 6, the overall manipulation success rate improves significantly when **MF** is  
299 used. When both **SALR** and **MF** are applied, the model achieves the best performance. These results  
300 highlight the importance of leveraging historical frame information and aligning vision-language  
301 embeddings with actions.

## 302 5 Conclusion

303 In this paper, we propose **HALO**, a vision-language-action (VLA) model designed to address the  
304 challenges of long-horizon robotic manipulation. We propose to use the Qwen2.5-VL to effectively  
305 process the historical frames and capture the long-dependencies. To balance the complexity and  
306 performance, we further design a selective spatial-temporal sampling strategy to fuse the long  
307 historical frames and current multi-view images. Besides, to bridge the modality gap between the  
308 actions and vision-language embeddings, we propose the state-aware latent re-representation to fuse  
309 their features and then use the aligned embeddings to guide the prediction of future actions. Extensive  
310 experiments demonstrate that our model outperforms existing VLA models in task performance, with  
311 greater advantages in long-horizon tasks.

## 312 References

- 313 [1] An Yang, Baosong Yang, Beichen Zhang, Binyuan Hui, Bo Zheng, Bowen Yu, Chengyuan  
314 Li, Dayiheng Liu, Fei Huang, Haoran Wei, et al. Qwen2.5 technical report. *arXiv preprint*  
315 *arXiv:2412.15115*, 2024.
- 316 [2] Zhe Chen, Weiyun Wang, Yue Cao, Yangzhou Liu, Zhangwei Gao, Erfei Cui, Jinguo Zhu, Shen-  
317 glong Ye, Hao Tian, Zhaoyang Liu, et al. Expanding performance boundaries of open-source  
318 multimodal models with model, data, and test-time scaling. *arXiv preprint arXiv:2412.05271*,  
319 2024.
- 320 [3] Shengding Hu, Yuge Tu, Xu Han, Chaoqun He, Ganqu Cui, Xiang Long, Zhi Zheng, Yewei  
321 Fang, Yuxiang Huang, Weilin Zhao, et al. Minicpm: Unveiling the potential of small language  
322 models with scalable training strategies. *arXiv preprint arXiv:2404.06395*, 2024.

- 323 [4] Moo Jin Kim, Karl Pertsch, Siddharth Karamcheti, Ted Xiao, Ashwin Balakrishna, Suraj Nair,  
 324 Rafael Rafailov, Ethan Foster, Grace Lam, Pannag Sanketi, et al. Openvla: An open-source  
 325 vision-language-action model. *arXiv preprint arXiv:2406.09246*, 2024.
- 326 [5] Kevin Black, Noah Brown, Danny Driess, Adnan Esmail, Michael Equi, Chelsea Finn, Niccolo  
 327 Fusai, Lachy Groom, Karol Hausman, Brian Ichter, et al.  $\pi$ 0: A vision-language-action flow  
 328 model for general robot control, 2024. URL <https://arxiv.org/abs/2410.24164>.
- 329 [6] Ruijie Zheng, Yongyuan Liang, Shuaiyi Huang, Jianfeng Gao, Hal Daumé III, Andrey Kolobov,  
 330 Furong Huang, and Jianwei Yang. Tracevla: Visual trace prompting enhances spatial-temporal  
 331 awareness for generalist robotic policies. *arXiv preprint arXiv:2412.10345*, 2024.
- 332 [7] Qixiu Li, Yaobo Liang, Zeyu Wang, Lin Luo, Xi Chen, Mozheng Liao, Fangyun Wei, Yu Deng,  
 333 Sicheng Xu, Yizhong Zhang, et al. Cogact: A foundational vision-language-action model for  
 334 synergizing cognition and action in robotic manipulation. *arXiv preprint arXiv:2411.19650*,  
 335 2024.
- 336 [8] Junjie Wen, Minjie Zhu, Yichen Zhu, Zhibin Tang, Jimming Li, Zhongyi Zhou, Chengmeng Li,  
 337 Xiaoyu Liu, Yixin Peng, Chaomin Shen, et al. Diffusion-vla: Scaling robot foundation models  
 338 via unified diffusion and autoregression. *arXiv preprint arXiv:2412.03293*, 2024.
- 339 [9] Junjie Wen, Yichen Zhu, Jimming Li, Minjie Zhu, Zhibin Tang, Kun Wu, Zhiyuan Xu, Ning Liu,  
 340 Ran Cheng, Chaomin Shen, et al. Tinyvla: Towards fast, data-efficient vision-language-action  
 341 models for robotic manipulation. *IEEE Robotics and Automation Letters*, 2025.
- 342 [10] Quan Vuong, Sergey Levine, Homer Rich Walke, Karl Pertsch, Anikait Singh, Ria Doshi,  
 343 Charles Xu, Jianlan Luo, Liam Tan, Dhruv Shah, et al. Open x-embodiment: Robotic learning  
 344 datasets and rt-x models. In *Towards Generalist Robots: Learning Paradigms for Scalable Skill  
 345 Acquisition@ CoRL2023*, 2023.
- 346 [11] Qingwen Bu, Jisong Cai, Li Chen, Xiuqi Cui, Yan Ding, Siyuan Feng, Shenyuan Gao, Xindong  
 347 He, Xu Huang, Shu Jiang, et al. Agibot world colosseo: A large-scale manipulation platform  
 348 for scalable and intelligent embodied systems. *arXiv preprint arXiv:2503.06669*, 2025.
- 349 [12] Brianna Zitkovich, Tianhe Yu, Sichun Xu, Peng Xu, Ted Xiao, Fei Xia, Jialin Wu, Paul  
 350 Wohlhart, Stefan Welker, Ayzaan Wahid, et al. Rt-2: Vision-language-action models transfer  
 351 web knowledge to robotic control. In *Conference on Robot Learning*, pages 2165–2183. PMLR,  
 352 2023.
- 353 [13] Siddharth Karamcheti, Suraj Nair, Ashwin Balakrishna, Percy Liang, Thomas Kollar, and Dorsa  
 354 Sadigh. Prismatic vlms: Investigating the design space of visually-conditioned language models.  
 355 In *Forty-first International Conference on Machine Learning*, 2024.
- 356 [14] Lucas Beyer, Andreas Steiner, André Susano Pinto, Alexander Kolesnikov, Xiao Wang, Daniel  
 357 Salz, Maxim Neumann, Ibrahim Alabdulmohsin, Michael Tschannen, Emanuele Bugliarello,  
 358 et al. Paligemma: A versatile 3b vlm for transfer. *arXiv preprint arXiv:2407.07726*, 2024.
- 359 [15] Jonathan Ho, Ajay Jain, and Pieter Abbeel. Denoising diffusion probabilistic models. *Advances  
 360 in neural information processing systems*, 33:6840–6851, 2020.
- 361 [16] Jiaming Song, Chenlin Meng, and Stefano Ermon. Denoising diffusion implicit models. *arXiv  
 362 preprint arXiv:2010.02502*, 2020.
- 363 [17] William Peebles and Saining Xie. Scalable diffusion models with transformers. In *Proceedings  
 364 of the IEEE/CVF international conference on computer vision*, pages 4195–4205, 2023.
- 365 [18] Cheng Chi, Zhenjia Xu, Siyuan Feng, Eric Cousineau, Yilun Du, Benjamin Burchfiel, Russ  
 366 Tedrake, and Shuran Song. Diffusion policy: Visuomotor policy learning via action diffusion.  
 367 *The International Journal of Robotics Research*, page 02783649241273668, 2023.
- 368 [19] Moritz Reuss, Jyothish Pari, Pulkit Agrawal, and Rudolf Lioutikov. Efficient diffusion trans-  
 369 former policies with mixture of expert denoisers for multitask learning. *arXiv preprint  
 370 arXiv:2412.12953*, 2024.

- 371 [20] Octo Model Team, Dibya Ghosh, Homer Walke, Karl Pertsch, Kevin Black, Oier Mees, Sudeep  
372 Dasari, Joey Hejna, Tobias Kreiman, Charles Xu, et al. Octo: An open-source generalist robot  
373 policy. *arXiv preprint arXiv:2405.12213*, 2024.
- 374 [21] Songming Liu, Lingxuan Wu, Bangguo Li, Hengkai Tan, Huayu Chen, Zhengyi Wang, Ke Xu,  
375 Hang Su, and Jun Zhu. Rdt-1b: a diffusion foundation model for bimanual manipulation. *arXiv*  
376 *preprint arXiv:2410.07864*, 2024.
- 377 [22] Jiazhao Zhang, Kunyu Wang, Rongtao Xu, Gengze Zhou, Yicong Hong, Xiaomeng Fang,  
378 Qi Wu, Zhizheng Zhang, and He Wang. Navid: Video-based vlm plans the next step for  
379 vision-and-language navigation. *arXiv preprint arXiv:2402.15852*, 2024.
- 380 [23] Qingwen Bu, Yanting Yang, Jisong Cai, Shenyuan Gao, Guanghui Ren, Maoqing Yao, Ping  
381 Luo, and Hongyang Li. Univla: Learning to act anywhere with task-centric latent actions. *arXiv*  
382 *preprint arXiv:2505.06111*, 2025.
- 383 [24] Stephen James and Andrew J Davison. Q-attention: Enabling efficient learning for vision-based  
384 robotic manipulation. *IEEE Robotics and Automation Letters*, 7(2):1612–1619, 2022.
- 385 [25] Mohit Shridhar, Lucas Manuelli, and Dieter Fox. Perceiver-actor: A multi-task transformer for  
386 robotic manipulation. In *Conference on Robot Learning*, pages 785–799. PMLR, 2023.
- 387 [26] Yunhai Feng, Jiaming Han, Zhuoran Yang, Xiangyu Yue, Sergey Levine, and Jianlan Luo.  
388 Reflective planning: Vision-language models for multi-stage long-horizon robotic manipulation.  
389 *arXiv preprint arXiv:2502.16707*, 2025.
- 390 [27] Shichao Fan, Quantao Yang, Yajie Liu, Kun Wu, Zhengping Che, Qingjie Liu, and Min  
391 Wan. Diffusion trajectory-guided policy for long-horizon robot manipulation. *arXiv preprint*  
392 *arXiv:2502.10040*, 2025.
- 393 [28] Jessica Borja-Diaz, Oier Mees, Gabriel Kalweit, Lukas Hermann, Joschka Boedecker, and  
394 Wolfram Burgard. Affordance learning from play for sample-efficient policy learning. In *2022*  
395 *International Conference on Robotics and Automation (ICRA)*, pages 6372–6378. IEEE, 2022.
- 396 [29] Shuai Bai, Keqin Chen, Xuejing Liu, Jialin Wang, Wenbin Ge, Sibo Song, Kai Dang, Peng Wang,  
397 Shijie Wang, Jun Tang, et al. Qwen2. 5-vl technical report. *arXiv preprint arXiv:2502.13923*,  
398 2025.
- 399 [30] Abby O'Neill, Abdul Rehman, Abhiram Maddukuri, Abhishek Gupta, Abhishek Padalkar,  
400 Abraham Lee, Acorn Pooley, Agrim Gupta, Ajay Mandlekar, Ajinkya Jain, et al. Open x-  
401 embodiment: Robotic learning datasets and rt-x models: Open x-embodiment collaboration 0.  
402 In *2024 IEEE International Conference on Robotics and Automation (ICRA)*, pages 6892–6903.  
403 IEEE, 2024.
- 404 [31] Xuanlin Li, Kyle Hsu, Jiayuan Gu, Karl Pertsch, Oier Mees, Homer Rich Walke, Chuyuan Fu,  
405 Ishikaa Lunawat, Isabel Sieh, Sean Kirmani, et al. Evaluating real-world robot manipulation  
406 policies in simulation. *arXiv preprint arXiv:2405.05941*, 2024.
- 407 [32] Bo Liu, Yifeng Zhu, Chongkai Gao, Yihao Feng, Qiang Liu, Yuke Zhu, and Peter Stone. Libero:  
408 Benchmarking knowledge transfer for lifelong robot learning. *Advances in Neural Information*  
409 *Processing Systems*, 36:44776–44791, 2023.
- 410 [33] Oier Mees, Lukas Hermann, Erick Rosete-Beas, and Wolfram Burgard. Calvin: A benchmark  
411 for language-conditioned policy learning for long-horizon robot manipulation tasks. *IEEE*  
412 *Robotics and Automation Letters*, 7(3):7327–7334, 2022.
- 413 [34] Anthony Brohan, Noah Brown, Justice Carbajal, Yevgen Chebotar, Joseph Dabis, Chelsea Finn,  
414 Keerthana Gopalakrishnan, Karol Hausman, Alex Herzog, Jasmine Hsu, et al. Rt-1: Robotics  
415 transformer for real-world control at scale. *arXiv preprint arXiv:2212.06817*, 2022.
- 416 [35] Delin Qu, Haoming Song, Qizhi Chen, Yuanqi Yao, Xinyi Ye, Yan Ding, Zhigang Wang,  
417 JiaYuan Gu, Bin Zhao, Dong Wang, et al. Spatialvla: Exploring spatial representations for  
418 visual-language-action model. *arXiv preprint arXiv:2501.15830*, 2025.

- 419 [36] Corey Lynch and Pierre Sermanet. Language conditioned imitation learning over unstructured  
420 data. *arXiv preprint arXiv:2005.07648*, 2020.
- 421 [37] Oier Mees, Lukas Hermann, and Wolfram Burgard. What matters in language conditioned  
422 robotic imitation learning over unstructured data. *IEEE Robotics and Automation Letters*,  
423 7(4):11205–11212, 2022.
- 424 [38] Suraj Nair, Aravind Rajeswaran, Vikash Kumar, Chelsea Finn, and Abhinav Gupta. R3m: A  
425 universal visual representation for robot manipulation. *arXiv preprint arXiv:2203.12601*, 2022.
- 426 [39] Xinghang Li, Minghuan Liu, Hanbo Zhang, Cunjun Yu, Jie Xu, Hongtao Wu, Chilam Cheang,  
427 Ya Jing, Weinan Zhang, Huaping Liu, et al. Vision-language foundation models as effective  
428 robot imitators. *arXiv preprint arXiv:2311.01378*, 2023.

